Brain Struct Funct (2015) 220:37–46
DOI 10.1007/s00429-013-0634-3

ORIGINAL ARTICLE

Dynamic brain functional connectivity modulated by resting-state networks

Xin Di · Bharat B. Biswal

Received: 5 March 2013 / Accepted: 31 August 2013 / Published online: 29 September 2013

Abstract Studies of large-scale brain functional connectivity using the resting-state functional magnetic resonance imaging have advanced our understanding of human brain functions. Although the evidence of dynamic functional connectivity is accumulating, the variations of functional connectivity over time have not been well characterized. In the present study, we aimed to associate the variations of functional connectivity with the intrinsic activities of resting-state networks during a single resting-state scan by comparing functional connectivity differences between when a network had higher and lower intrinsic activities. The activities of the salience network, default mode network (DMN), and motor network were associated with changes of resting-state functional connectivity. Higher activity of the salience network was accompanied by greater functional connectivity between the fronto-parietal regions and the DMN regions, and between the regions within the DMN. Higher DMN activity was associated with less connectivity between the regions within the DMN, and greater connectivity between the regions within the fronto-parietal network. Higher motor network activity was correlated with greater connectivity between the regions within the motor network, and smaller connectivity between the DMN regions and fronto-parietal regions, and between the DMN regions and the motor regions. In addition, the whole brain network modularity was positively correlated with the motor network activity, suggesting that the brain is more segregated as sub-systems when the motor network is intrinsically activated. Together, these results demonstrate the association between the resting-state connectivity variations and the intrinsic activities of specific networks, which can provide insights on the dynamic changes in large-scale brain connectivity and network configurations.

Keywords Default mode network · Dynamic connectivity · fMRI · Nonlinear connectivity · Resting-state · Salience network

Introduction

Studies of localization of specific brain regions and their association to cognitive and affective functions have shaped our understanding of the human brain. Recent studies of large-scale brain networks using the resting-state functional magnetic resonance imaging (fMRI) have provided novel insights on how distributed brain regions are functionally integrated (e.g., Biswal et al. 1995, 2010; Fox et al. 2005). Generally, studies on the functional connectivity are based upon the temporal correlations between spatially remote neurophysiological events (Friston 1994) with an implicit assumption that the functional connectivity is constant during the observation period. Recent studies demonstrate that the functional connectivity (Allen et al. 2012; Chang and Glover 2010; Handwerker et al. 2012) as well as the spatial extent of the resting-state networks (Kang et al. 2011; Kiviniemi et al. 2011) can vary periodically. However, the dynamic changes in functional connectivity have hitherto been overlooked in fMRI studies most likely due to the poor temporal resolution of fMRI.

Electronic supplementary material The online version of this article (doi:10.1007/s00429-013-0634-3) contains supplementary material, which is available to authorized users.

X. Di · B. B. Biswal (✉)
Department of Biomedical Engineering,
New Jersey Institute of Technology, University Height,
607 Fenster Hall, Newark, NJ 07102, USA
e-mail: bbiswal@gmail.com

Given that dynamic changes in connectivity have been well documented in electroencephalography (EEG) and magnetoencephalography (MEG) studies (Dimitriadis et al. 2012; Rubinov et al. 2009), there is a need to study the dynamic changes in functional connectivity during the resting-state.

To better understand the dynamic changes in functional connectivity, it is critical to identify the factors that modulate the functional connectivity. Vanhaudenhuyse and colleagues used a behavioral sampling method to demonstrate that the awareness of the environment or of self varies at an approximate frequency of 0.05 Hz, which is similar to the low-frequency fluctuations that are typically observed in the resting-state fMRI (Vanhaudenhuyse et al. 2011). Most interestingly, these fluctuations associated with awareness of self were positively and negatively correlated with the activities of the default mode network (DMN) and task positive network, respectively, and vice versa for the fluctuations associated with awareness of the environment. As it is difficult to monitor the mental state during the resting-state fMRI scan, Fan and colleagues proposed that recording the skin conductance response during fMRI can reflect psychophysiological states of autonomic arousal. They demonstrated that the functional connectivity during the resting-state was modulated by autonomic arousal (Fan et al. 2012). Similarly, we hypothesize that changes in the intrinsic activities (low versus high activities) may reflect the changes in mental state and therefore be used as an index to determine whether the mental state modulates the functional connectivity. Specifically, we divided the fMRI images into two conditions based upon the low and high intrinsic activities of a particular network. This analysis strategy is similar to the recent ideas of point process analysis or spontaneous event-related process (Liu and Duyn 2013; Tagliazucchi et al. 2012; Wu et al. 2013); however, our analysis provides a mean to associate the changes in the intrinsic activities of a specific network to the changes in functional connectivity that may extend to other brain systems.

In the present study, we systematically investigated whether and how the functional connectivity changes across the whole brain were associated with different brain network activities. Spatial independent component analysis (ICA) was first used to identify brain networks (Beckmann et al. 2005). Functional connectivity between 160 regions of interest (ROIs) was then calculated separately when a network had high or low activities. We characterized the functional connectivity using simple correlation coefficient and network properties based on the graph theory (Bullmore and Sporns 2009). Therefore, we not only investigated single connections that were correlated with network activity, but also studied how the whole brain integration and segregation were correlated with network activity.

We were particularly interested in the networks that were related to the resting-state functions such as the DMN and salience network (Seeley et al. 2007) among the commonly studied resting-state networks (Cole et al. 2010). The DMN regions exhibit higher energy consumption and neural activity during the resting-state (Raichle et al. 2001; Shulman et al. 1997), and receive information from widely distributed brain regions (Liao et al. 2010; Yan and He 2011). The salience network is suggested to be critical when switching (activating and deactivating) different brain networks (Sridharan et al. 2008). Our hypothesis is that higher salience network activity would be correlated with increased functional connectivity and network efficiency of large-scale brain networks, while higher DMN activity would be correlated with decreased functional connectivity and network efficiency of brain networks.

Materials and methods

MRI data set

The resting-state fMRI and anatomical MRI dataset was derived from the Beijing_Zang dataset of the 1,000 functional connectomes project (http://fcon_1000.projects.nitrc.org/) (Biswal et al. 2010) (Biswal et al. 2010). This dataset originally included 198 subjects. Only 191 subject data remained after removing data due to large head motion, poor coverage, or failure of image registration. The current analysis only used the last one-third of the subjects ($n = 63$, 35F/28 M). The mean age of these subjects was 21.3 years (range from 18 to 25 years). The MRI data were scanned using a SIEMENS Trio 3-Tesla scanner at Beijing Normal University. Two hundred and thirty resting-state functional images were acquired for each subject with TR of 2 s. The resolution of the fMRI images was $3.125 \times 3.125 \times 3$ mm with $64 \times 64 \times 36$ voxels. The T1-weighted three-dimensional magnetization-prepared rapid gradient echo (MPRAGE) image was acquired using the following parameters: 128 slices, TR = 2,530 ms, TE = 3.39 ms, slice thickness = 1.33 mm, flip angle = 7°, inversion time = 1,100 ms, FOV = 256×256 mm^2.

Data analysis overview

The data analysis strategy is illustrated in Fig. 1. After preprocessing, spatial ICA was first performed on the fMRI data to identify resting-state networks. For each network of interest, the correspondent time course was used to divide the time points into two groups: higher and lower activity of the network. The time courses of 160 ROIs across whole brain were then divided into two sets according to the

network activity separation. Correlation differences among the 160 ROIs were compared between the two sets, and subsequent network analysis was also performed.

Functional MRI preprocessing

The resting-state fMRI images were preprocessed using the SPM8 package (http://www.fil.ion.ucl.ac.uk/spm/) under MATLAB 7.6 environment. After discarding the first two images of each subject, the remaining functional images were motion corrected and co-registered to the subject's own high-resolution anatomical image. For all the subjects included in the current analysis, the largest head motion parameters were smaller than 2 mm or 2°. The anatomical images were then normalized to the T1 template provided by SPM8, which was in the Montreal Neurological Institute (MNI) space. The parameters of anatomical image normalization were then applied to the functional images to normalize them into the MNI space. At this step, all the functional images were resampled into $3 \times 3 \times 3$ mm^3 voxel size. Finally, all the functional images were spatially smoothed using a Gaussian kernel with 8 mm full-width at half-maximum (FWHM). In addition, the anatomical images were segmented using the new segment routine in SPM8 to generate subject specific white matter (WM) and cerebrospinal fluid (CSF) masks.

Spatial ICA

Spatial ICA was conducted using the Group ICA of fMRI Toolbox (GIFT) (Calhoun et al. 2001). Preprocessed resting-state fMRI images were concatenated across all subjects and fed into the GIFT toolbox. Twenty ICs were extracted. The resulting IC maps were visually examined to identify meaningful resting-state networks described in earlier studies (Biswal et al. 2010; Cole et al. 2010). Nine out of twenty components were considered as meaningful resting-state networks, which included the DMN, salience, attention, left and right executive, motor, primary and extrastriate visual and auditory networks (Fig. 2).

Functional ROIs

Coordinates of 160 ROIs using a series of meta-analyses were obtained from Dosenbach et al. (2010). Spherical ROIs were defined with a radius of 8 mm. Mean time series from the ROIs were extracted for each subject.

Time series processing

The six rigid-body motion parameters, the first eigenvector of WM, and the first eigenvector of CSF were regressed out from the time series of 9 resting-state networks and 160 ROIs using a linear regression model. The WM and CSF masks were defined for each subject by thresholding the segmented WM and CSF images at $p > 0.99$. All the time series were then band-pass filtered at 0.01–0.1 Hz, and z-transformed into z-score time series.

Modularity analysis

A modularity analysis was conducted using the Louvain modularity algorithm to assign the ROIs into different brain systems (Blondel et al. 2008; Rubinov and Sporns

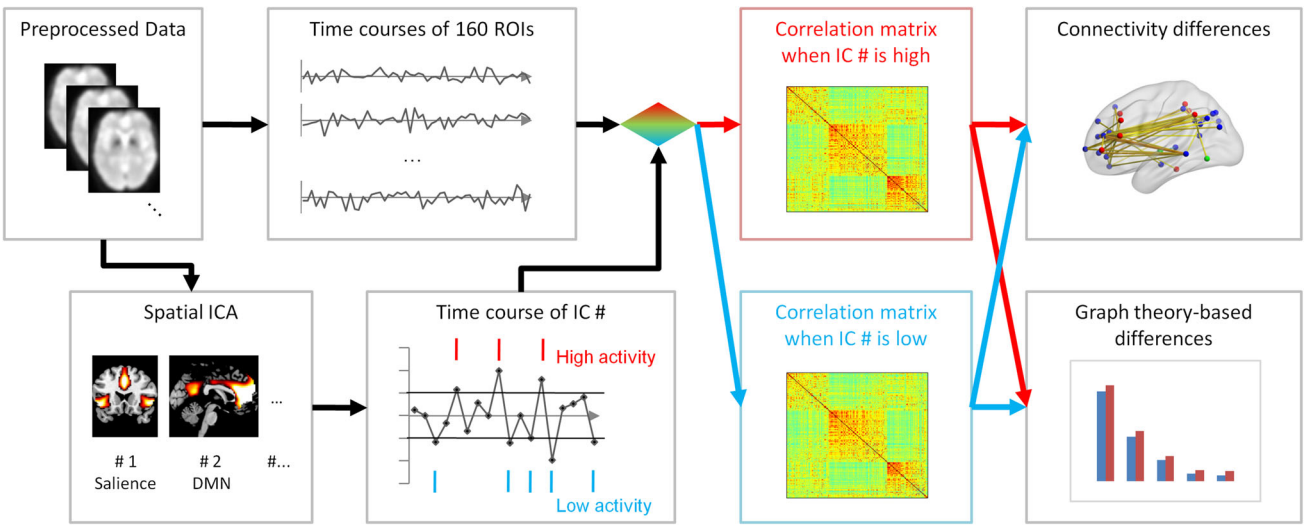

Fig. 1 Flow chart of data analysis. The critical step of data analysis is that the time course of a particular IC was used to separate the time series of 160 ROIs according to the IC's activity. Time points when the IC has higher 1/3 activity and lower 1/3 activity were grouped into two sets, and correlation matrices and network properties of these two sets were compared subsequently. *Arrows* and *characters* in *red* indicate when a network has higher activity, while *blue color* indicates when a network has lower activity

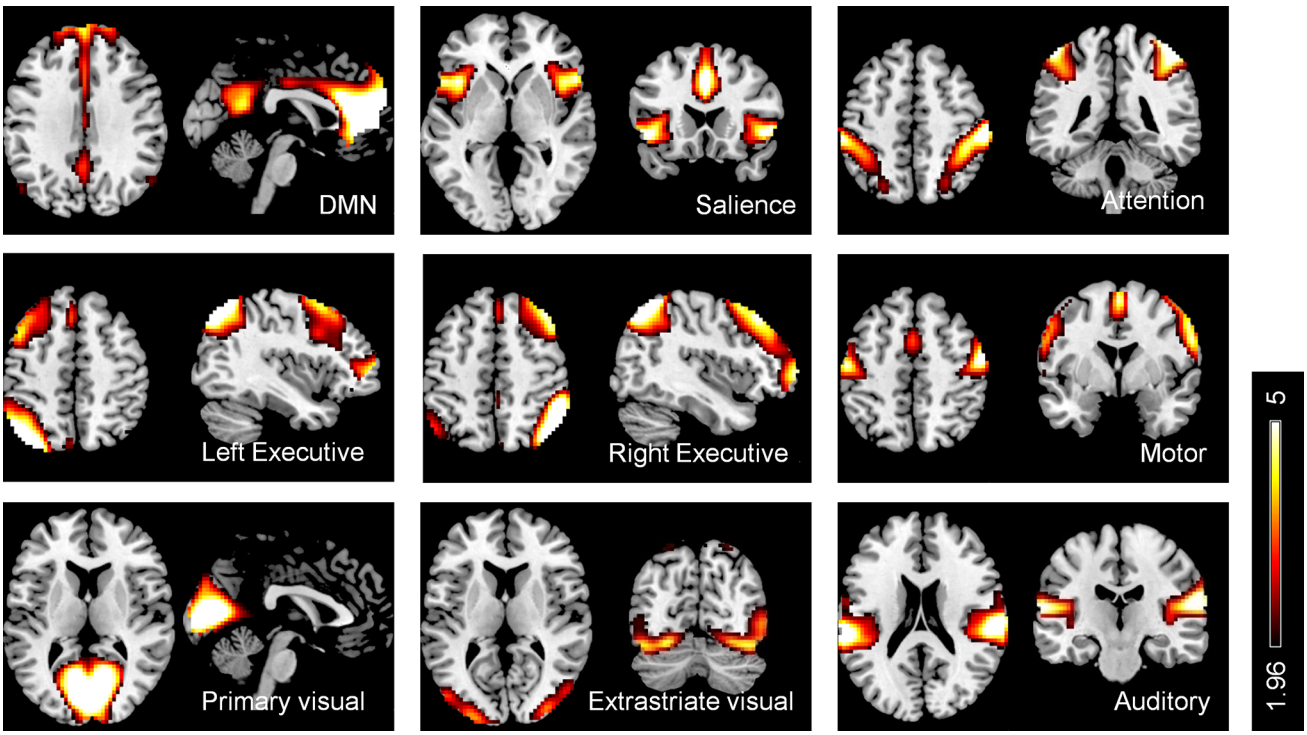

Fig. 2 Resting-state networks used in the time points separation analysis, which were identified by spatial ICA. The IC maps were spatially z transformed, and thresholded at $z > 1.96$

2011). The modularity analysis was based on the mean correlation matrix between 160 time series. This algorithm takes into account both positive and negative weights of the network edges and avoids biased thresholding of the networks. This analysis identified three modules for the 160 ROIs: the default mode module, the fronto-parietal module, and the visuomotor module (supplementary Figure S1). The number of modules is smaller than six, which was originally reported by Dosenbach et al. (2010), most likely due to the differences in image preprocessing steps and modularity algorithm. We adopted the three modules solution to roughly classify these ROIs into either DMN or task positive networks. Other task-positive networks, such as the executive control and dorsal attention networks, are difficult to separate because these networks are vulnerable to preprocessing steps as well as different mental states (Spreng et al. 2013).

Time points separation analysis

Z-transformed time series of each subject from each of the nine networks were divided into two data sets based on the amplitude of the time points. The time point with greater than a z-value of 0.43 (upper 33 %) was categorized into the high activity dataset, whereas the time point with less than −0.43 (lower 33 %) were stratified into the low activity dataset. On average, a single data set comprised of 76 time points. The time points separating analysis was performed separately for each of the nine networks. We also conducted time point separation based on upper 50 % and lower 50 % z-values. The subsequent analysis generally gave similar results but with less statistical significance. Therefore, we only report the results of the upper and lower 33 % separation.

Comparison of connectivity matrices

The correlation matrices of a given resting-state network during high or low activity were initially transformed into Fisher's z scores. Then, we used a paired t test to compare the differences in correlation values between high and low activities for each pair of ROIs. We used a threshold of $p < 0.0056$ (0.05/9) to correct for multiple comparisons of the nine resting-state network. Then, a false discovery rate (FDR) correction was used for each analysis to correct for multiple comparisons of correlations (12,720 edges). The connections that showed significant changes of functional connectivity were visualized using the BrainNet Viewer toolbox (http://www.nitrc.org/projects/bnv/). Given that the multiple comparison correction may be too stringent, we used a less stringent correction threshold that corrected for only the number of edges to illustrate general trends of functional connectivity changes. These results are reported in the supplementary materials section.

Comparison of network properties

In addition to the individual correlation coefficients, we also compared the graph theory-based measures, which characterize the whole brain functional segregation and integration (Bullmore and Sporns 2009). These network properties included modularity (Newman 2006), mean clustering coefficients, and global efficiency (Watts and Strogatz 1998). Modularity estimates the extent the whole network is segregated into sub-communities. The clustering coefficient measures the efficiency of the local information transmission of every node, whereas the global efficiency measures the information transmission efficiency of the entire network. Binary unidirectional networks were built for each condition and for each subject by thresholding the absolute correlation matrices to maintain 10, 20 and 30 % of connections (a.k.a., sparsity). These sparsities were chosen because the brain network was typically fallen within this range (Achard and Bullmore 2007; He et al. 2008). Network measures were calculated using the brain connectivity toolbox (Rubinov and Sporns 2010). Differences between high and low activity of these network parameters were compared using a paired t test. FDR correction was applied to a total of 27 comparisons (3 sparsity $\times$ 3 networks $\times$ 3 parameters).

Results

Out of the nine networks, three networks were associated with significant functional connectivity changes at the threshold of $p < 0.05$ after correction for the number of edges and networks, including the salience network, DMN, and motor network. We observed no significant association between changes in functional connectivity and network activities for the other six networks at the threshold of $p < 0.05$ after correcting for the number of edges and networks.

The salience network

The connectivity changes related to the salience network activity are visualized in Fig. 3. Forty-eight connections were positively associated with the salience network activity. A set of connections that exhibited differences in functional connectivity between the regions of the fronto-parietal module which were mainly located in the lateral prefrontal and parietal regions, and the regions of the default mode module which were mainly located in the medial prefrontal cortex and the left inferior temporal lobule. Another set of connections that showed differences in functional connectivity was mainly among the regions within the default mode module. Using a less stringent threshold, an obvious pattern is observable in the functional connectivity difference matrix (the right panel of the supplementary Figure S2A). These connections that revealed positive association with the salience network activity appeared to be predominantly left lateralized (Fig. 3); however, when using a less stringent threshold, the lateralized pattern was unclear (supplementary Figure S3). In contrast, there was only one connection between the left middle insula and the right temporal region that was negatively correlated with the salience network activity. None of the modularity, mean clustering coefficient, and global efficiency measures at the three sparsity levels was associated with the salience network activity (Fig. 4a).

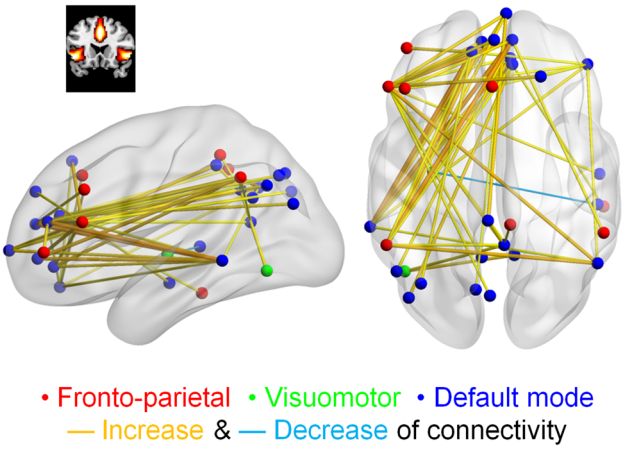

Fig. 3 Functional connectivity differences associated with the salience network activity. Differences were thresholded at $p < 0.05$ after correction for the number of edges and networks

The DMN

The functional connectivity changes related to the DMN activity are shown in Fig. 5. Ten functional connections revealed weaker functional connectivity when the DMN exhibited higher compared with lower activity. These connections were mainly between the posterior cingulate cortex (PCC) of the default mode module with other regions of the default mode module. When we applied a less stringent threshold, we observed that the decrease in functional connectivity was also among other regions of the default mode module, including the medial prefrontal cortex (supplementary Figure S2 and S4). In contrast, seven connections exhibited increased functional connectivity when the DMN was higher than lower, mainly between the regions in the fronto-parietal module. When using a less stringent threshold, it was more apparent that the increased functional connectivity was mainly between the fronto-parietal regions, and between the cerebellar and the default mode regions (Figure S4). Lastly, the global efficiency was positively associated with the DMN activity

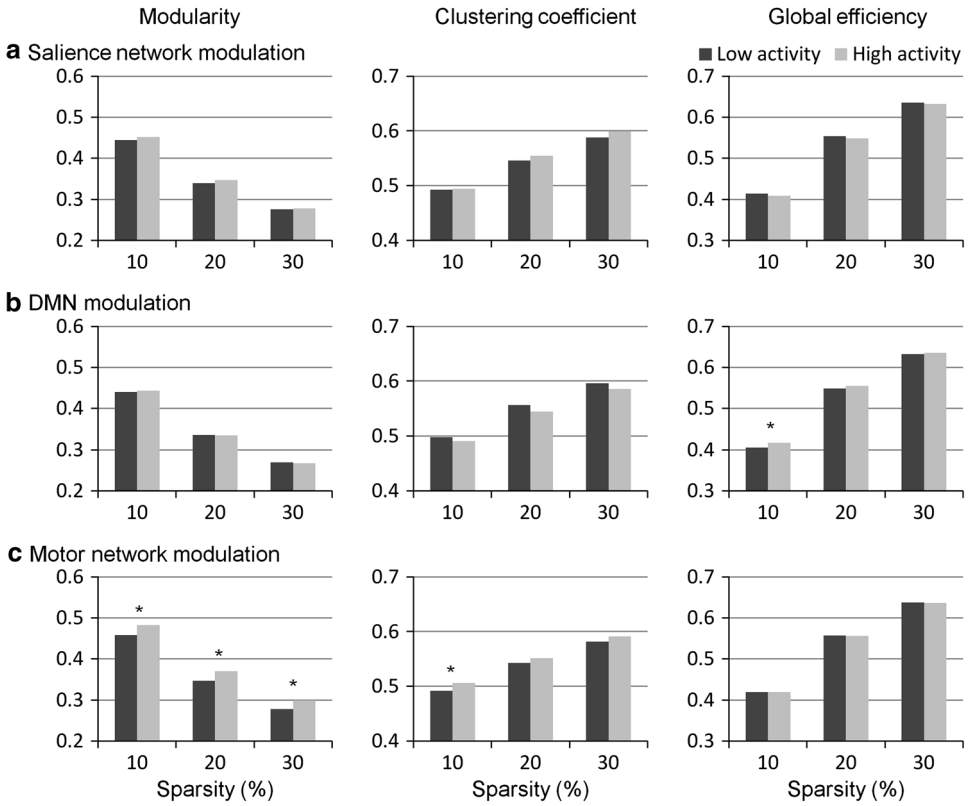

Fig. 4 Network properties associated with the intrinsic activities of the salience network (**a**), DMN (**b**), and motor network (**c**), respectively. *$p < 0.05$ after FDR correction for all the 27 comparisons

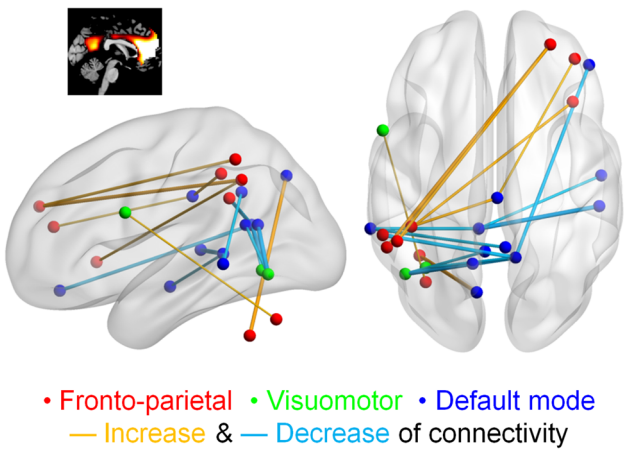

Fig. 5 Functional connectivity differences associated with the DMN activity. Differences were thresholded at $p < 0.05$ after correction for the number of edges and networks

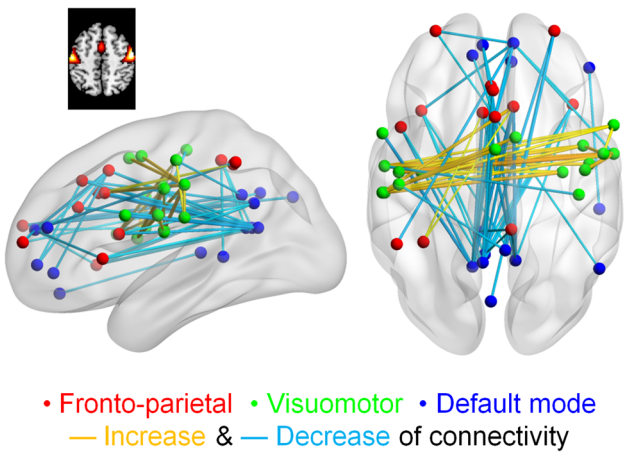

Fig. 6 Functional connectivity differences associated with the motor network activity. Differences were thresholded at $p < 0.05$ after correction for the number of edges and networks

at the sparsity level of 10 % (Fig. 4b). Specifically, the global efficiency was 0.011 higher when the DMN activity was higher ($t = 3.05$, SD $= 0.030$, $p = 3.40 \times 10^{-3}$).

The motor network

The functional connectivity changes related to the motor network activity are illustrated in Fig. 6. Twenty-six connections demonstrated higher functional connectivity when the motor network exhibited higher activity. These regions involved mainly the bilateral sensorimotor regions. In contrast, 43 connections showed lower functional connectivity when the motor network had higher activity, which were between the regions in the default mode module and the regions in the fronto-parietal module, and between the regions in the default mode module and the regions in the visuomotor module. These patterns were more obvious when using a less stringent threshold (Figure S2 and S5).

In addition, the motor network activity was also associated with the network properties (Fig. 4c). For all the sparsity levels tested, the modularity was higher when the motor network exhibited high activity. At the sparsity of 10, 20, and 30 % the modularity was 0.025 ($t = 3.46$, SD = 0.058, $p = 9.82 \times 10^{-4}$), 0.023 ($t = 4.17$, SD = 0.044, $p = 9.49 \times 10^{-5}$), and 0.021 ($t = 4.08$, SD = 0.041, $p = 1.33 \times 10^{-4}$) greater, respectively, when the motor network exhibited high activity. Lastly, the mean clustering coefficient was 0.14 higher when the motor network activity was high at the sparsity level of 10 % ($t = 3.78$, SD = 0.030, $p = 3.60 \times 10^{-4}$).

Discussion

The current study systematically examined the association between the resting-state functional connectivity and the intrinsic activities of the different resting-state networks by separating the time points into high and low intrinsic activities. Three of the nine networks, including the salience, the DMN, and the motor networks, demonstrated associations between their intrinsic activities and the resting-state functional connectivity. In addition, network properties were also observed to be associated with the intrinsic activities of different brain networks.

The salience network

The salience network generally comprises of the bilateral anterior insula and the anterior cingulate cortex, and was first distinguished from other task-positive networks by Seeley and colleagues (Seeley et al. 2007). The salience network is involved in bottom-up detection of salience events, and plays a key role in switching between large-scale networks to facilitate the access of resources from attention and working memory (Menon and Uddin 2010). One of the roles of the anterior insula was to activate the executive network and deactivate the DMN across visual, auditory modalities and in the resting-state as revealed by Granger causality analysis (Sridharan et al. 2008). Our result demonstrates that the high activity of the salience network is associated with increased functional connectivity between the default mode and fronto-parietal executive networks. This result suggests that the salience network not only modulates the activities of the two networks, but may also modulate the relationships between them. Given that the causal relationship between the salience network activity and the changes of functional connectivity is difficult to infer, an alternative explanation may be that the increased synchrony among these regions in the default mode and fronto-parietal modules yields higher salience network activity. The former explanation is more plausible, because the regions in the salience network are generally the driving hubs of the whole brain, which sends information to various regions of the whole brain (Sridharan et al. 2008; Yan and He 2011). Furthermore, the salience network contains a special type of neurons termed von Economo neurons, which have large axons to facilitate rapid relay of salience network signals to other brain regions (Allman et al. 2005, 2010; Cauda et al. 2013). This type of neuron may support the special function of the salience network during modulation of large-scale brain networks.

The current results also reveal an association between the salience network activity and the functional connectivity between the regions within the default mode module. Together with the previous Granger causality studies showing that the salience network regions are mainly the driving hubs, whereas the DMN regions are generally the driven hubs of the brain (Sridharan et al. 2008; Yan and He 2011), these evidences suggest that the salience network may modulate the DMN integration. This association is in line with a recent finding that demonstrates a correlation between the salience network white matter integrity and DMN functions (Bonnelle et al. 2012). Even though the subjects are in the resting-state, the salience network continuously monitors salience events in other sensory modalities including autonomic arousal (Critchley et al. 2000; Fan et al. 2012). As reported by Fan and colleagues, the association between increased DMN functional connectivity and increased skin conductance response (Fan et al. 2012) may be partially explained by the association between the increased DMN functional connectivity and increased salience network activity in our current result.

The DMN

The DMN, mainly comprised of the PCC/precuneus, medial prefrontal cortex, and bilateral inferior parietal lobe, was first defined by Raichle and colleagues based on the observation that this set of brain regions showed higher energy consumption during the resting-state compared with when performing tasks (Raichle et al. 2001). The regions in this network are usually deactivated during task execution (Laird et al. 2009; Shulman et al. 1997), and their activities are anticorrelated with task positive regions during the resting-state (Fox et al. 2005). Surprisingly, the current study demonstrates that the increase in DMN activity is mainly accompanied by smaller functional connectivity between the regions within the default mode module. The decrease of within-DMN functional connectivity extends to other regions in the default mode modules when using a less stringent threshold (Supplementary Figure S4). This is in contrast with the finding from other networks, e.g., the motor network, where the network activity is positively

associated with the within-network functional connectivity. One possible explanation of the negative correlation may be that the DMN is heterogeneous, and is comprised of different fractions (Andrews-Hanna et al. 2010; Laird et al. 2009); thus, the increased DMN activity is accompanied by relative independence of these sub-networks within the DMN to support heterogeneous functions.

Increased activity of the DMN is positively associated with wide spread functional connectivity between the regions in the fronto-parietal module, and between the default mode and the cerebellar regions. However, the connections that conveyed increased functional connectivity did not show a clear pattern (the right panel of Figure S2B) as compared with those in the salience and the motor network (the right panels of Figure S2A and S2C). Network analysis further reveals that the increase of functional connectivity may result in higher global efficiency that facilitates global information transmission. This may suggest that higher internal oriented state as indexed by higher DMN intrinsic activity (Vanhaudenhuyse et al. 2011) may be associated with high integration across the whole brain. However, we note that the increase of global efficiency was only observed at the specific sparsity level of 10 %, and therefore, these effects warrant future studies.

The motor network

The motor network activity was positively covaried with the functional connectivity between the motor network regions, while negatively correlated with the functional connectivity between the default mode and the fronto-parietal regions, and between the default mode and the visuomotor regions. The associations between the motor network activity and within-motor network synchronization is reasonable, and is in line with the studies showing that performing of a motor task is accompanied by both the activations of the motor areas and increase in functional connectivity between them (e.g., Zhuang et al. 2005). However, it is interesting to observe that the functional connectivity decreases between regions from different brain systems when the motor network activity increases, especially between the default mode and the fronto-parietal regions, and between the default mode and the visuomotor regions. Further, graph theory-based analysis reveals that the modularity of the whole brain network increases at all the three sparsity levels, and the mean clustering coefficient increases at the sparsity level of 10 % as the motor network activity increases. These results suggest that the brain network is more segregated as independent modules and more locally organized when the motor network has higher intrinsic activity (Bullmore and Sporns 2009). Thus, we show within a single resting-state session, network reconfiguration occurs to facilitate local information processing and suppress information from other systems. Whether the same network configuration will occur when subjects explicitly perform a motor task needs further in-depth exploration.

Dynamic connectivity

In addition to the recent findings that showed dynamic functional connectivity in the resting-state (Allen et al. 2012; Chang and Glover 2010; Handwerker et al. 2012), the current study demonstrates that the variations of resting-state functional connectivity are correlated with the activity of other networks. The current results suggest a functional significance of the dynamic functional connectivity, and motivate theories based upon the dynamics of connectivity to explain complex brain function. In addition, the framework presented in the current analysis may be used to understand the mechanisms underlying mental disorders, such as schizophrenia (Menon 2011; Palaniyappan and Liddle 2012). For example, alterations of the salience network structures and functions (Chan et al. 2011; Palaniyappan and Liddle 2012) and impaired functional connectivity between the DMN and the central executive network (Manoliu et al. 2013a, b) were both observed in patients with schizophrenia. The present results directly revealed a link between the salience network activity and the functional connectivity between the DMN and the fronto-parietal regions, which may shed light on the mechanism of schizophrenia.

One outcome of dynamic connectivity is the reconfiguration of brain networks. In addition to previous studies showing brain network reconfiguration during learning or different cognitive loads (Bassett et al. 2011; Kitzbichler et al. 2011), the current study reveals for the first time that whole brain network properties, especially the modularity, varied within a single resting-state scan session. The link between modularity changes and the activity of a specific network may provide new insight on the dynamic organization of the brain network. Further in-depth analyses of whether modularity structures or hub organizations change during the resting-state are needed. The method used in the present study provides a framework to study network reconfigurations in resting-state as well as conventional task fMRI data.

Lastly, the method adopted in the present study is only an approximate measure of modulation effects. Such method is limited by both statistical power and causal inferences. More sophisticated models such as nonlinear dynamic causal model (DCM) (Friston et al. 2003; Seghier and Friston 2013; Stephan et al. 2008), and Granger causality (Goebel et al. 2003; Liao et al. 2009, 2010, 2011) may be used in the future to study dynamic connectivity to provide a more accurate and valuable causal information of the modulation effects.

Acknowledgments This study was supported by a National Institute of Health grant 5R01AG032088. We thank Suril Gohel and Dr. Eun H. Kim for discussions on data analysis and comments on an earlier version of this manuscript.

References

Achard S, Bullmore E (2007) Efficiency and cost of economical brain functional networks. PLoS Comput Biol 3:e17. doi:10.1371/journal.pcbi.0030017

Allen EA, Damaraju E, Plis SM, et al. (2012) Tracking whole-brain connectivity dynamics in the resting state. Cereb cortex (New York, NY: 1991). doi:10.1093/cercor/bhs352

Allman JM, Watson KK, Tetreault NA, Hakeem AY (2005) Intuition and autism: a possible role for Von Economo neurons. Trends Cogn Sci 9:367–373. doi:10.1016/j.tics.2005.06.008

Allman JM, Tetreault NA, Hakeem AY et al (2010) The von Economo neurons in frontoinsular and anterior cingulate cortex in great apes and humans. Brain Struct Funct 214:495–517. doi:10.1007/s00429-010-0254-0

Andrews-Hanna JR, Reidler JS, Sepulcre J et al (2010) Functional-anatomic fractionation of the brain's default network. Neuron 65:550–562

Bassett DS, Wymbs NF, Porter MA et al (2011) Dynamic reconfiguration of human brain networks during learning. Proc Natl Acad Sci USA 108:7641–7646. doi:10.1073/pnas.1018985108

Beckmann CF, DeLuca M, Devlin JT, Smith SM (2005) Investigations into resting-state connectivity using independent component analysis. Philos Trans R Soc Lond B Biol Sci 360:1001–1013. doi:10.1098/rstb.2005.1634

Biswal B, Yetkin FZ, Haughton VM, Hyde JS (1995) Functional connectivity in the motor cortex of resting human brain using echo-planar MRI. Magn Reson Med: Off J Soc Magn Reson Med/Soc Magn Reson Med 34:537–541. doi:10.1002/mrm.1910340409

Biswal BB, Mennes M, Zuo X-N et al (2010) Toward discovery science of human brain function. Proc Natl Acad Sci USA 107:4734–4739. doi:10.1073/pnas.0911855107

Blondel VD, Guillaume J-L, Lambiotte R, Lefebvre E (2008) Fast unfolding of communities in large networks. J Stat Mech: Theory Exp 2008:P10008. doi:10.1088/1742-5468/2008/10/P10008

Bonnelle V, Ham TE, Leech R, et al. (2012) Salience network integrity predicts default mode network function after traumatic brain injury. Proc Natl Acad Sci 109(12):4690–4695. doi:10.1073/pnas.1113455109

Bullmore E, Sporns O (2009) Complex brain networks: graph theoretical analysis of structural and functional systems. Nat Rev Neurosci 10:186–198. doi:10.1038/nrn2575

Calhoun VD, Adali T, Pearlson GD, Pekar JJ (2001) A method for making group inferences from functional MRI data using independent component analysis. Hum Brain Mapp 14:140–151

Cauda F, Torta DME, Sacco K et al (2013) Functional anatomy of cortical areas characterized by Von Economo neurons. Brain Struct Funct 218:1–20. doi:10.1007/s00429-012-0382-9

Chan RCK, Di X, McAlonan GM, Gong Q (2011) Brain anatomical abnormalities in high-risk individuals, first-episode, and chronic schizophrenia: an activation likelihood estimation meta-analysis of illness progression. Schizophr Bull 37:177–188. doi:10.1093/schbul/sbp073

Chang C, Glover GH (2010) Time-frequency dynamics of resting-state brain connectivity measured with fMRI. NeuroImage 50:81–98. doi:10.1016/j.neuroimage.2009.12.011

Cole DM, Smith SM, Beckmann CF (2010) Advances and pitfalls in the analysis and interpretation of resting-state FMRI data. Frontiers Syst Neurosci 4:8. doi:10.3389/fnsys.2010.00008

Critchley HD, Elliott R, Mathias CJ, Dolan RJ (2000) Neural activity relating to generation and representation of galvanic skin conductance responses: a functional magnetic resonance imaging study. J Neurosci 20:3033–3040

Dimitriadis SI, Laskaris NA, Tsirka V et al (2012) An EEG study of brain connectivity dynamics at the resting state. Nonlinear Dynamics, Psychol Life Sci 16:5–22

Dosenbach NUF, Nardos B, Cohen AL et al (2010) Prediction of individual brain maturity using fMRI. Science (New York, NY) 329:1358–1361. doi:10.1126/science.1194144

Fan J, Xu P, Van Dam NT et al (2012) Spontaneous brain activity relates to autonomic arousal. J Neurosci 32:11176–11186

Fox MD, Snyder AZ, Vincent JL et al (2005) The human brain is intrinsically organized into dynamic, anticorrelated functional networks. Proc Natl Acad Sci USA 102:9673–9678

Friston KJ (1994) Functional and effective connectivity in neuroimaging: a synthesis. Hum Brain Mapp 2:56–78. doi:10.1002/hbm.460020107

Friston KJ, Harrison L, Penny W (2003) Dynamic causal modelling. NeuroImage 19:1273–1302

Goebel R, Roebroeck A, Kim D-S, Formisano E (2003) Investigating directed cortical interactions in time-resolved fMRI data using vector autoregressive modeling and Granger causality mapping. Magn Reson Imaging 21:1251–1261

Handwerker DA, Roopchansingh V, Gonzalez-Castillo J, Bandettini PA (2012) Periodic changes in fMRI connectivity. NeuroImage. doi:10.1016/j.neuroimage.2012.06.078

He Y, Chen Z, Evans A (2008) Structural insights into aberrant topological patterns of large-scale cortical networks in Alzheimer's disease. J Neurosci: Off J Soc Neurosci 28:4756–4766. doi:10.1523/JNEUROSCI.0141-08.2008

Kang J, Wang L, Yan C et al (2011) Characterizing dynamic functional connectivity in the resting brain using variable parameter regression and Kalman filtering approaches. NeuroImage 56:1222–1234. doi:10.1016/j.neuroimage.2011.03.033

Kitzbichler MG, Henson RNA, Smith ML et al (2011) Cognitive effort drives workspace configuration of human brain functional networks. J Neurosci: Off J Soc Neurosci 31:8259–8270. doi:10.1523/JNEUROSCI.0440-11.2011

Kiviniemi V, Vire T, Remes J et al (2011) A sliding time-window ICA reveals spatial variability of the default mode network in time. Brain Connect 1:339–347. doi:10.1089/brain.2011.0036

Laird AR, Eickhoff SB, Li K et al (2009) Investigating the functional heterogeneity of the default mode network using coordinate-based meta-analytic modeling. J Neurosci: Off J Soc Neurosci 29:14496–14505. doi:10.1523/JNEUROSCI.4004-09.2009

Liao W, Marinazzo D, Pan Z et al (2009) Kernel Granger causality mapping effective connectivity on FMRI data. IEEE Trans Med Imaging 28:1825–1835. doi:10.1109/TMI.2009.2025126

Liao W, Mantini D, Zhang Z et al (2010) Evaluating the effective connectivity of resting state networks using conditional Granger causality. Biol Cybern 102:57–69

Liao W, Ding J, Marinazzo D et al (2011) Small-world directed networks in the human brain: multivariate Granger causality analysis of resting-state fMRI. NeuroImage 54:2683–2694. doi:10.1016/j.neuroimage.2010.11.007

Liu X, Duyn JH (2013) Time-varying functional network information extracted from brief instances of spontaneous brain activity. Proc Natl Acad Sci 110(11):4392–4397. doi:10.1073/pnas.1216856110

Manoliu A, Riedl V, Doll A et al (2013a) Insular dysfunction reflects altered between-network connectivity and severity of negative symptoms in schizophrenia during psychotic remission. Frontiers Humn Neurosci. doi:10.3389/fnhum.2013.00216

Manoliu A, Riedl V, Zherdin A, et al. (2013b) Aberrant dependence of default mode/central executive network interactions on

anterior insular salience network activity in Schizophrenia. Schizophr Bull. doi:10.1093/schbul/sbt037
Menon V (2011) Large-scale brain networks and psychopathology: a unifying triple network model. Trends Cogn Sci 15:483–506. doi:10.1016/j.tics.2011.08.003
Menon V, Uddin LQ (2010) Saliency, switching, attention and control: a network model of insula function. Brain Struct Funct 214:655–667. doi:10.1007/s00429-010-0262-0
Newman MEJ (2006) Modularity and community structure in networks. Proc Natl Acad Sci USA 103:8577–8582. doi:10.1073/pnas.0601602103
Palaniyappan L, Liddle PF (2012) Does the salience network play a cardinal role in psychosis? An emerging hypothesis of insular dysfunction. J Psychiatry Neurosci: JPN 37:17–27. doi:10.1503/jpn.100176
Raichle ME, MacLeod AM, Snyder AZ et al (2001) A default mode of brain function. Proc Natl Acad Sci USA 98:676–682. doi:10.1073/pnas.98.2.676
Rubinov M, Sporns O (2010) Complex network measures of brain connectivity: uses and interpretations. NeuroImage 52:1059–1069. doi:10.1016/j.neuroimage.2009.10.003
Rubinov M, Sporns O (2011) Weight-conserving characterization of complex functional brain networks. NeuroImage 56:2068–2079. doi:10.1016/j.neuroimage.2011.03.069
Rubinov M, Knock SA, Stam CJ et al (2009) Small-world properties of nonlinear brain activity in schizophrenia. Hum Brain Mapp 30:403–416. doi:10.1002/hbm.20517
Seeley WW, Menon V, Schatzberg AF et al (2007) Dissociable intrinsic connectivity networks for salience processing and executive control. J Neurosci: Off J Soc Neurosci 27:2349–2356. doi:10.1523/JNEUROSCI.5587-06.2007
Seghier ML, Friston KJ (2013) Network discovery with large DCMs. NeuroImage 68:181–191. doi:10.1016/j.neuroimage.2012.12.005
Shulman GL, Fiez JA, Corbetta M et al (1997) Common blood flow changes across visual tasks: II. decreases in cerebral cortex. J Cogn Neurosci 9:648–663. doi:10.1162/jocn.1997.9.5.648
Spreng RN, Sepulcre J, Turner GR et al (2013) Intrinsic architecture underlying the relations among the default, dorsal attention, and frontoparietal control networks of the human brain. J Cogn Neurosci 25:74–86. doi:10.1162/jocn_a_00281
Sridharan D, Levitin DJ, Menon V (2008) A critical role for the right fronto-insular cortex in switching between central-executive and default-mode networks. Proc Natl Acad Sci USA 105:12569–12574. doi:10.1073/pnas.0800005105
Stephan KE, Kasper L, Harrison LM et al (2008) Nonlinear dynamic causal models for fMRI. NeuroImage 42:649–662. doi:10.1016/j.neuroimage.2008.04.262
Tagliazucchi E, Balenzuela P, Fraiman D, Chialvo DR (2012) Criticality in large-scale brain FMRI dynamics unveiled by a novel point process analysis. Frontiers Physiol 3:15. doi:10.3389/fphys.2012.00015
Vanhaudenhuyse A, Demertzi A, Schabus M et al (2011) Two distinct neuronal networks mediate the awareness of environment and of self. J Cogn Neurosci 23:570–578. doi:10.1162/jocn.2010.21488
Watts DJ, Strogatz SH (1998) Collective dynamics of "small-world" networks. Nature 393:440–442. doi:10.1038/30918
Wu G-R, Liao W, Stramaglia S et al (2013) A blind deconvolution approach to recover effective connectivity brain networks from resting state fMRI data. Med Image Anal 17:365–374. doi:10.1016/j.media.2013.01.003
Yan C, He Y (2011) Driving and driven architectures of directed small-world human brain functional networks. PLoS ONE 6:e23460. doi:10.1371/journal.pone.0023460
Zhuang J, LaConte S, Peltier S et al (2005) Connectivity exploration with structural equation modeling: an fMRI study of bimanual motor coordination. NeuroImage 25:462–470. doi:10.1016/j.neuroimage.2004.11.007